[Supporting Information]

Piezopotential Gated Nanowire-Nanotube-Hybrid Field-Effect-Transistor

Weihua Liu[1,3†], *Minbaek Lee*[1†], *Lei Ding*[2], *Jie Liu*[2], *Zhong Lin Wang*[1*]

† Authors equally contributed.

[1]School of Material Science and Engineering, Georgia Institute of Technology, GA 30332, USA

[2] Department of Chemistry, Duke University, Durham, NC 27708, USA

[3] Department of Microelectronics, Xi'an Jiaotong University, Xi'an, Shaanxi 710049, China

† Authors equally contributed.

*Corresponding author: zhong.wang@mse.gatech.edu

Materials and Methods

Substrate preparation. Two types of substrates were employed in the device fabrication, Si (*p*++) (Wafer world inc.) and Kapton polyimide film (Model: HN500, DuPont) for typical back-gate SWNT FET and hybrid flexible FET, respectively. Si substrates have a resistivity in a range of 1-20 ohm·cm, and orientated in [*100*]. In case of Si substrates, silicon dioxide layer was firstly formed via thermal growth method with a thickness of 200 nm. The thickness of the Kapton film was 127 μm. All substrates were rinsed with acetone, isopropyl alcohol and DI water before the device fabrication process.

ZnO piezoelectric-fine-wire growth. The ZnO PFWs were grown via a vapor-solid process (1-2). ZnO powder was used as the source material and loaded in an alumina boat located at the center of an alumina tube, which was placed in a single-zone horizontal tube furnace. Argon gas was used as carrier gas at a flow rate of 50 sccm throughout the growth process. An alumina substrate with length of 10 cm was placed 20 cm downstream from the source material. The furnace was heated to 1475 °C and was held at that temperature for 4.5 h under a pressure of ~250 mbar. Then the furnace was turned off, and the tube was cooled down to room temperature under an argon flow.

Selective growth of SWNTs. The dense arrays of aligned SWNTs were grown on single-crystal ST-cut quartz substrates using an ethanol/methanol mixture as the carbon source and Cu nanoparticles as catalysts (19). SWNTs within the arrays revealed a narrow diameter distribution from 1.55 to 1.78 nm. The grown SWNTs are almost exclusively semiconducting, as proven by previous studies (3-4).

SWNT transfer. The transfer process was adapted from previous reports (3,5) with minor modifications. It consists of 8 steps as follows. 1) Spin-cast a drop of 6 % poly (methyl methacrylate) (950 K molecular weight) (PMMA) solution in anisole (from MICRO CHEM) on SWNTs/quartz at 4000 rpm for 50 sec to form a PMMA layer; 2) Bake the substrate at 170 ºC for 15 min; 3) Cut the PMMA film into 500 by 2000 μm pieces; 4) Immerse the PMMA/SWNTs/quartz substrate in preheated KOH (70 °C, 1 mol/L) aqueous solution for 1 h. The PMMA/SWNTs films were peeled off from the quartz substrate in this process; 5) Move the films from the KOH solution to DI water and rinse with DI water; 6) Attach PMMA film on target substrate, which have already had the first metal layer of the electrodes. By controlling direction of PMMA film, one can align SWNTs along two metal electrodes; 7) Bake the PMMA/SWNTs/Substrate at 170 ºC for 15 min; 8) Remove only PMMA layer by dipping the substrate gently into acetone for ~ 10 min followed by ethanol and D.I. water rinsing.

Electrical measurements. The electrical measurements of the fabricated devices were carried out using a semiconductor analyzer (Keithley 4200). The samples were mounted on the metal stage of a probe-station. In case of flexible hybrid FET, SWNT FET-embedded side of the Kapton substrate was fixed

on the stage and the other side served as a deformation site. The bending deformation was performed by three dimensional (3D) micromanipulator while the current signal was monitored continuously.

***I_{DS}-V_{DS}* characteristics of hybrid FET.**

I_{DS}-V_{DS} characteristics of hybrid FET was investigated depending on the deformation of hybrid device. After stretching ZnO piezoelectric fine wire, I_{DS}-V_{DS} curve was increased up to ~ 40 % at drain-source voltage of 1 V. Since ZnO gate generates only negative gate bias effectively, the increasing drain-source current indicates that the SWNT FET in hybrid device has negative transconductance around nearly zero gate bias. Here, asymmetric drain-source current changes were resulted from the deviation of the center position between SWNT FET channel and piezoelectric gate. This gives different gate bias to source and drain contact. All bending deformation was conducted with micromanipulator. Here, the estimated strain in ZnO PFW is ~ 0.05 %

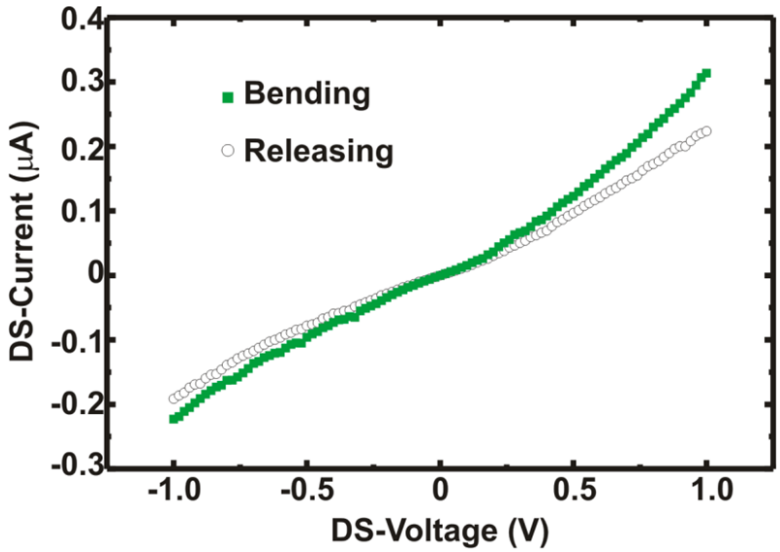

Figure S1. The changes of I_{DS}-V_{DS} characteristics of piezoelectric gated hybrid FET before and after applying a strain in the ZnO wire.

Sequent response to serial deformation on hybrid FET.

To investigate the relationship between external deformation and piezopotential on ZnO PFW, we measured drain-source current I_{DS} in the function of the strain in ZnO PFW on hybrid FET (Figure. S2). The 3-dimensional micromanipulator was utilized to bend step by step for three times and then released step by step as well. Drain-source current I_{DS} were measured under a fixed drain-source bias of 1 V. During a three steps of bending deformation, the I_{DS} increased from ~55 to ~110 nA in step-by-step with strain in PFW from ~0.05% to ~0.1 %. When the device was released in step-by-step, the I_{DS} recovered to its original level. However, asymmetric signal outputs between bending and releasing steps were observed. A plausible explanation can be two reasons as followed here. Firstly, originally SWNT FETs have hysteresis behavior to the gate voltage because of the charge trap between insulating oxide layer and SWNT surface as reported before (6). Secondly, flexible substrate has delayed deformation compared to external micromanipulator. It can explain relatively changing behavior after bending of releasing events.

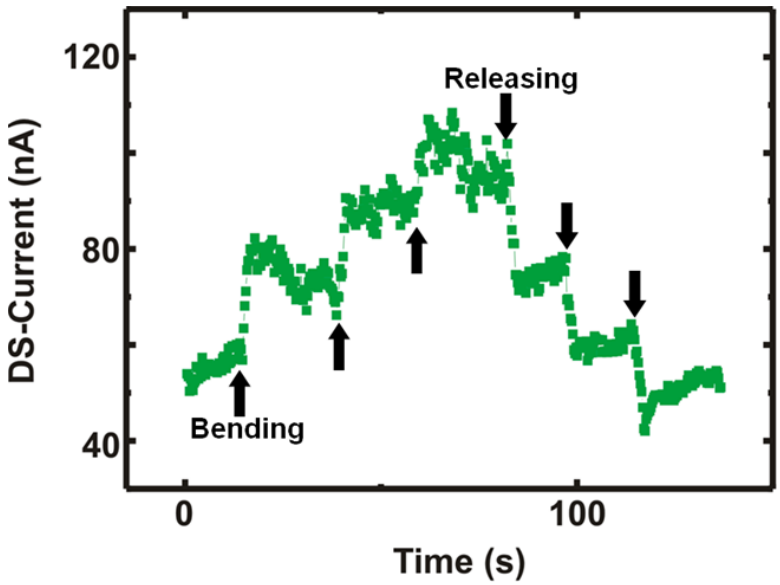

Figure S2. Drain source current of a hybrid FET at a fixed voltage by stepply changing the degree of bending (strain) in the ZnO PFW.

Estimation of tensile stain in ZnO PFW on flexible substrate

In all hybrid FET fabrications, 127-μm-thick Kapton film (HN 500, DuPont) served as substrate, which is relatively larger than the diameter of any ZnO PFWs (0.5 ~ 3 μm) we used in our experiments (see Figure. S3). Therefore, we can assume that the strain in the PFW is approximately equal to the strain of the site where it was placed on the surface of the Kapton substrate. The axial strain ε_{zz} along the length of the PFW is approximately (7)

$$\varepsilon_{zz} = 3\frac{a}{l}\frac{D_{max}}{l}\left(1-\frac{z}{l}\right)$$

where z is the distance measured from the fixed end of the Kapton substrate to the middle of the ZnO PFW; a is the half-thickness of the Kapton substrate; l is the length of Kapton film from the fixed end to the end of three dimensional micromanipulator; and D_{max} is the maximum deformation of the probe exerted to the Kapton substrate.

In our typical measurements, we placed a ZnO PFW and micromanipulator from the fixed point of Kapton substrate at 150 ~ 600 μm and 10 ~ 20 mm, respectively. Maximum deformation was ranged from ~100 μm to ~600 μm. The estimated strain was expected in range from ~0.05 % to ~0.1 %.

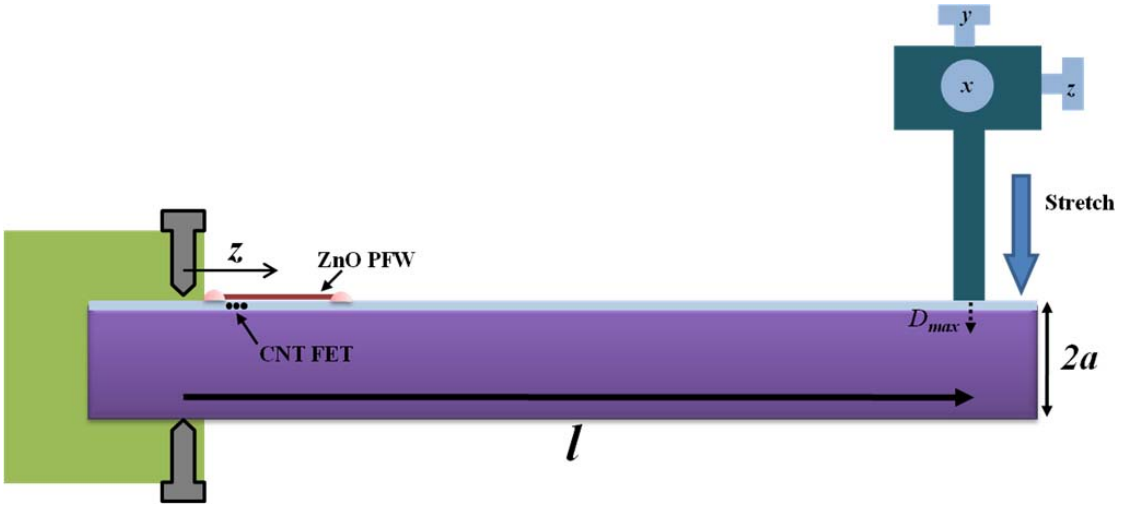

Figure S3. 3D micromanipulator for introducing mechanical strain in a FET along a particular direction. The strain was calculated based on the dimensions and the displacement of the tip part.

Control experiment using polycrystalline ZnO coated fiber.

We carried out control experiments to rule out possible artifacts other than piezoelectric effects (Figure. S4). Here, control samples were fabricated using polycrystalline ZnO film coated Kevlar 129 fiber. AC sputtering method was employed to deposit polycrystalline ZnO film on Kevlar 129 fiber. After then, the fibers were manually assembled on SWNT FET embedded Kapton substrate like the same structure of hybrid FETs reported here. By assembling polycrystalline ZnO film coated fiber instead of ZnO PFW, no macroscopic piezopotential was expected regardless any status of strain on the device. Periodic deformations were applied to fiber integrated FETs, while drain-source current I_{DS} was monitored by applying drain-source voltage V_{DS} of 1 V. To avoid any possibilities of FETs with least transconductance ($< |1\ nS|$) which originally shows no response to piezopotential, we employed fifteen control devices. Figure S4 shows representative current signals of measured control samples. All measured drain-source currents I_{DS} exhibited no response to any strain of polycrystalline ZnO film coated Kevlar fiber. Here, we applied a tensile strain to the fiber with 0.08 % in each measurement. This result also indicates that SWNT FETs, we used here, have least response to any strain itself or environments rather than ZnO PFW.

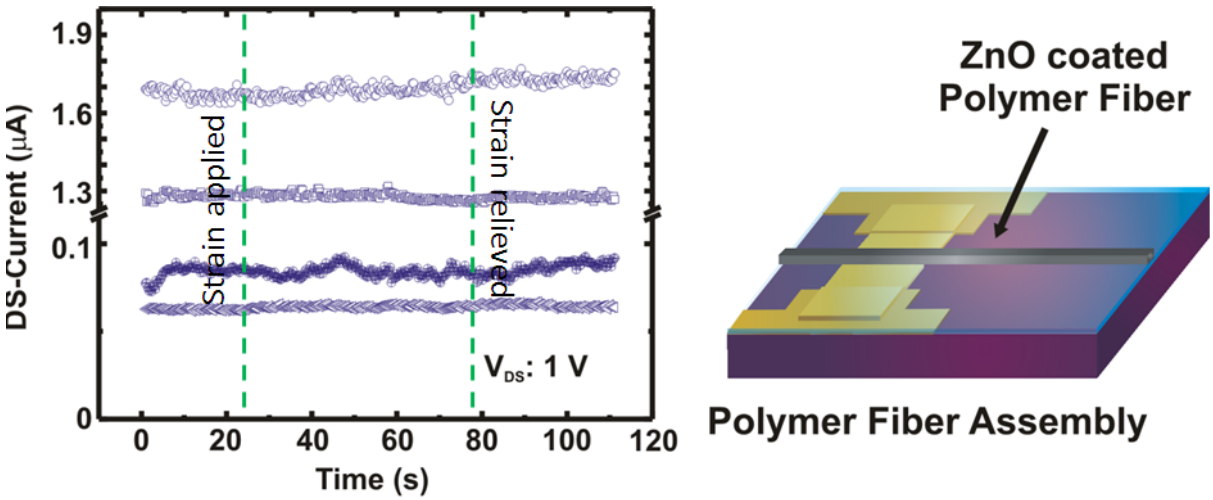

Figure S4. The performance of four hybrid FETs fabricated by replacing the ZnO PFWs by polymer fibers coated with polycrystalline ZnO, showing no response to the strain applied to the fiber.

Theoretical simulation.

COMSOL multiphysics version 3.4 was used in the simulation without considering the conductivity of ZnO. The material constants for ZnO used in the calculations are as follows: Young's modulus $\mathrm{E} = 129.0\ \mathrm{GPa}$, and Poisson ratio $\nu = 0.349$; relative dielectric constants $\kappa_{\perp}{}^{\mathrm{r}} = 7.77$, $\kappa_{\parallel}{}^{\mathrm{r}} = 8.91$, and the piezoelectric constants $\mathrm{e}_{31} = -0.51\ \mathrm{C/m^2}$, $\mathrm{e}_{33} = 1.22\ \mathrm{C/m^2}$, $\mathrm{e}_{15} = -0.45\ \mathrm{C/m^2}$ (8). To simulate the piezopotential along the C axis, the wire is fixed at the bot tom and free at top side. A pulling force f_z along the C axis is applied at the free end.

References

1. Pan, Z. W.; Dai, Z. R.; Wang, Z. L. *Science* **2001**, *291*, 1947.
2. Wang, Z. L. *MRS Bulletin* **2007**, *32*, 109.
3. Ding, L.; Tselev, A.; Wang, J.; Yuan, D.; Chu, H.; McNicholas, T. P.; Li, Y.; Liu J. *Nano Lett.* **2009**, *9*, 800.
4. Li, Y.; Cui, R.; Ding, L.; Liu, Y.; Zhou, W.; Zhang, Y.; Jin, Z.; Peng, F.; Liu J. *Adv. Mater.* **2010**, *22*, 1508.
5. Jiao, L.; Xian, X.; Wu, Z.; Zhang, J.; Liu, Z. *Nano Lett.* **2009**, *9*, 205.
6. Fuhrer, M.S.; Kim, B.M.; Du1rkop, T.; Brintlinger, T. **2002**, *2*, 755.
7. Soutas-Little R. W. *Elasticity, XVI, 431*; Dover Publications: Mineola, NY, 1999.
8. Gao, Y.F.; Wang, Z. L. *Nano Lett.* **2007**, *7*, 2499-2505.